


## Quantum limit cyclotron resonance in monolayer epitaxial graphene in magnetic fields up to 560 T: The relativistic electron and hole asymmetry

Daisuke Nakamura,<sup>1</sup> Hiroaki Saito,<sup>1</sup> Hiroki Hibino,<sup>2</sup> Kenichi Asano,<sup>3</sup> and Shojiro Takeyama <sup>1,\*</sup>

<sup>1</sup>The Institute for Solid State Physics, The University of Tokyo, Kashiwa, Chiba 277-8581, Japan

<sup>2</sup>NTT Basic Research Laboratories, NTT Corporation, Atsugi, Kanagawa 243-0198, Japan

and School of Science and Technology, Kwansei Gakuin University, Sanda, Hyogo 669-1337, Japan

<sup>3</sup>Center for Education in Liberal Arts and Sciences, Osaka University, Toyonaka, Osaka 560-0043, Japan



(Received 19 October 2018; accepted 4 February 2020; published 17 March 2020)

An ultrahigh-magnetic field cyclotron resonance in monolayer epitaxial graphene resolves split peaks in 300–500 T of the magnetic field, generated by the electromagnetic flux compression 1000-T-class megagauss generator. The peak splitting observed is most probably evidence of electron-hole symmetry breaking of Dirac relativistic electrons in graphene. Moreover, the observed asymmetry of absorption intensity between the split peaks is a strong indication of mode repulsion induced by the electron-electron correlation.

DOI: [10.1103/PhysRevB.101.115420](https://doi.org/10.1103/PhysRevB.101.115420)

Graphene is an ideal two-dimensional carbon honeycomb lattice, which exhibits physical properties reflecting the massless Dirac dispersion of electrons near the Fermi level. One of these properties is a half-integer quantum Hall effect [1] that stems from an unconventional  $n = 0$  Landau level (LL). In a parabolic electronic band based on the free-electron model, LLs develop linearly with the magnetic field  $B$ . This linear dependence is modified to a sublinear  $B$  dependence upon the introduction of a nonparabolicity of the electron bands. In this respect, the  $\sqrt{B}$  dependence of LLs in graphene can be regarded as a consequence of an extreme limit of the nonparabolicity, where a Landau quantization is observable even in magnetic fields as small as several mTs [2–4], signifying that a strong magnetic field limit is already achieved with the application of a moderate strength.

There have been a number of attempts at infrared magneto-optical spectroscopy of graphene [3–13]. Optical measurements have been able to resolve the cyclotron resonance (CR) between electron LLs, between hole LLs, and between a hole and an electron LL [3–13], whose transition energies were found to be proportional to  $\sqrt{B}$  reflected by their linear energy band dispersion. Nevertheless, the ratio between the different inter-LL transition energies does not obey that expected when the electron-electron ( $e$ - $e$ ) interaction is absent, thus implying the importance of the effect of this interaction. In fact, Kohn's theorem, which states that the CR is immune to the  $e$ - $e$  interaction, has not been contradicted [14]. In principle, Kohn's theorem is not necessarily applicable to graphene, whose electron energy displays a linear dispersion relation at around the  $K$  and  $K'$  points of the Brillouin zone. Moreover, the CR transition energy exhibits large and nonmonotonic shifts as a function of the LL filling factor in the exfoliated monolayer graphene [9]; these shifts are claimed to stem from the splitting of the  $n = 0$  LL induced by the  $e$ - $e$  interaction. For instance, the  $n = 0$

LL splitting gap observed in the transport measurements was believed to be originated from the  $e$ - $e$  interaction [15,16], as similarly seen for a high-resolution magnetotunneling spectroscopy [17]. All these works have been conducted in graphene samples of low-electron concentration and of high carrier mobility, and those phenomena have not been fully comprehended and are still a topic under theoretical debate.

By contrast, for an industrial application of potential requirements of large-area devices, graphene growth by epitaxy [18] or by chemical vapor deposition (CVD) [19] is indispensable, despite the disadvantage of lower-mobility characteristics compared to that of the exfoliated graphene. In addition, high carrier doping is an important factor for electro-optical device applications, and reduction of carrier mobility is inexorable by doping processes. Low-mobility graphene requires a high-magnetic field to observe quantum oscillations that implicate important information for basic electronic properties. A high-magnetic field environment offers high-energy resolution to the CR spectra, as the cyclotron energy  $\hbar\omega_c$  overwhelms the spectral broadening  $\hbar/\tau$  even at room temperature, and further allows CR transitions involving  $n = 0 \rightarrow +1$  and  $n = -1 \rightarrow 0$  to be measured simultaneously, as the filling factor satisfies  $-2 < \nu < 2$  that extends to heavily doped samples with carrier density as high as  $10^{12}$ – $10^{13}$  cm<sup>-2</sup>. Nonetheless, there are only a few experimental studies on CRs in epitaxial or CVD graphene under high-magnetic-field conditions. Booshehri *et al.* observed the room-temperature CR spectra in the low-mobility large-area monolayer graphene grown by CVD under magnetic fields reaching 170 T [12]. They found distinct CR spectra of  $n = 0 \rightarrow +1$  and  $n = -1 \rightarrow 0$  simultaneous transitions, owing to the substantial reduction of the carrier concentration after a thermal annealing treatment.

The epitaxial monolayer graphene used in this study was prepared by a thermal decomposition method [20–22]. Results of the micro-Raman mapping, which utilizes the characteristic Raman shift to obtain the number of graphene layers, revealed a 70–80% of the sample area covered with monolayer

\*takeyama@issp.u-tokyo.ac.jp

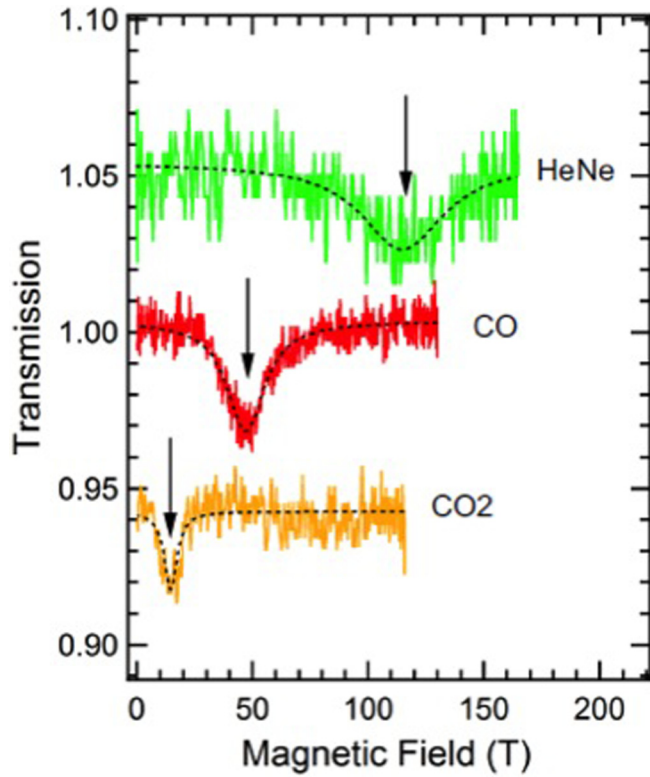


FIG. 1. CR transmission spectra in magnetic fields by various laser light sources. Measurements carried out at room temperature via the STC megagauss generator.

graphene, as supported by an atomic force microscope image showing almost 80% of the area covered with monolayer graphene. (The corresponding details are provided in the Supplemental Material [23].) The carrier density and the mobility of the graphene sample were determined by the van der Pauw transport measurements to be  $n_e = 3 \times 10^{11} \text{ cm}^{-2}$  and  $\mu = 3 \times 10^3 \text{ cm}^2/\text{Vs}$ , respectively.

A single-turn coil (STC) ultrahigh-magnetic-field generator system [24] was used to produce a magnetic field reaching until approximately 200 T using a coil of 10-mm bore. Magnetic fields stronger than 200 T can be generated by the electromagnetic flux compression (EMFC) generator system [25–27]. For the magneto-optical measurements, several types of light source were employed for mapping the Landau-level fan chart. For the STC, linearly polarized infrared lasers with  $\text{CO}_2$  (wavelength  $\lambda = 9\text{--}11 \mu\text{m}$ ),  $\text{CO}$  ( $\lambda = 5.2\text{--}5.7 \mu\text{m}$ ), and  $\text{HeNe}$  ( $\lambda = 3.39 \mu\text{m}$ ) gases were used. The measurement setup is detailed in our report [28]. For measurements in the EMFC system, a thulium fiber laser ( $\lambda = 1950 \text{ nm}$ ) was used as the incident laser; as its spectral width was as broad as 50 nm, a monochromator was used to choose a wavelength with 5-nm in spectral width. The entire experimental setup is described in the Supplemental Material [23].

A wide range of magnetic field (to approximately 600 T) was available for the CR experiments, while, accordingly, the resonance photon energies ranged from near-infrared to infrared. Figure 1 demonstrates the CR transmission spectra measured using different laser sources in magnetic fields of up to 160 T, produced by a STC megagauss generator. The

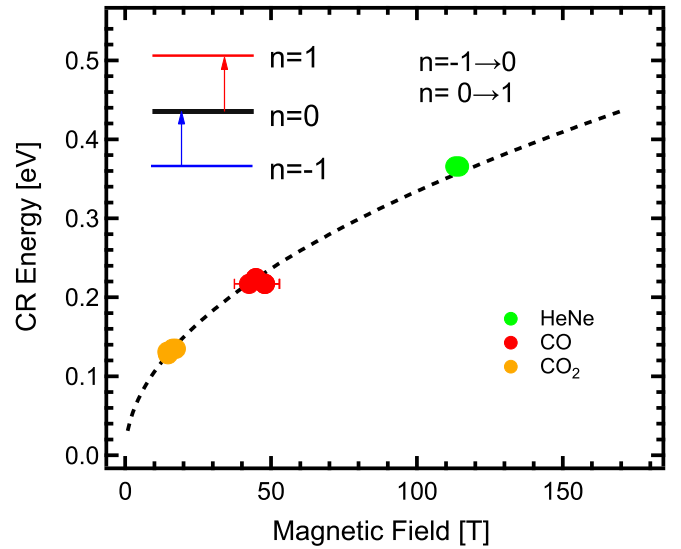


FIG. 2. CR energies in magnetic fields obtained from Fig. 1. CR positions follow the  $\sqrt{B}$  (dashed) line arising from  $n = 0 \rightarrow 1$  and  $n = -1 \rightarrow 0$  transitions. The inset illustrates the allowed CR transition involved.

spectra showed a slightly asymmetric profile, and the formula by Abergel and Fal'ko [29],

$$T(B) \propto 1 - \frac{\frac{\sqrt{B_c}}{\tau}}{\left(\frac{\sqrt{B_c}}{B} - 1\right)^2 + \left(\frac{1}{\tau}\right)^2}, \quad (1)$$

where  $T(B)$ ,  $B_c$ , and  $\tau$  express the transmission, the resonance field, and the relaxation time of an electron, respectively, reproduced their overall profiles. From the figure, note that the asymmetry of the CR absorption spectrum becomes more noticeable with the increasing resonance magnetic field.

Figure 2 displays the plots of CR resonance peaks, representing two degenerate CRs' transitions of  $n = 0 \rightarrow 1$  and  $-1 \rightarrow 0$ , obtained through the different incident lasers. A couple of facts justify this assignment. First, the Fermi velocity obtained by the LL fan chart fitting (the dashed line in Fig. 2) of the relation,  $E = v_F \sqrt{2e\hbar B}$  (where  $-e$  is the electron charge), gave a reasonable value of  $v_F = 0.92 \times 10^6 \text{ m/s}$ . Second, as the photon energy of the incident light became larger than that of the  $\text{CO}_2$  laser (130 meV), the CR transitions between the adjacent LLs were restricted to only those of  $n = 0 \rightarrow +1$  and  $n = -1 \rightarrow 0$ . In other words, the filling factor should be less than 2, or  $\nu = 2\pi\hbar n_e/eB < 2$ , at the magnetic field  $B$ , satisfying  $E = v_F \sqrt{2e\hbar B} > 130 \text{ meV}$ . This relation leads to  $E_F < v_F \sqrt{e\hbar B} = 92 \text{ meV}$ , whose value does not contradict  $E_F = \hbar v_F \sqrt{\pi n_e} = 50 \text{ meV}$ , estimated from the electron density,  $n_e = 3 \times 10^{11} \text{ cm}^{-2}$ , determined from the transport measurements.

Measurements in the EMFC ended up with an explosive destruction of a magnet coil, including the sample and its holders, just after the peak magnetic field was achieved. Figures 3(a) and 3(b) present the plots of the CR transmission spectra against the magnetic field and the corresponding results, for the 2-mm cut (from the same 10 mm  $\times$  10 mm square flake) samples A1 and A2, respectively. The resonance photon energies were 626.2 meV ( $\lambda = 1980 \text{ nm}$ ) and

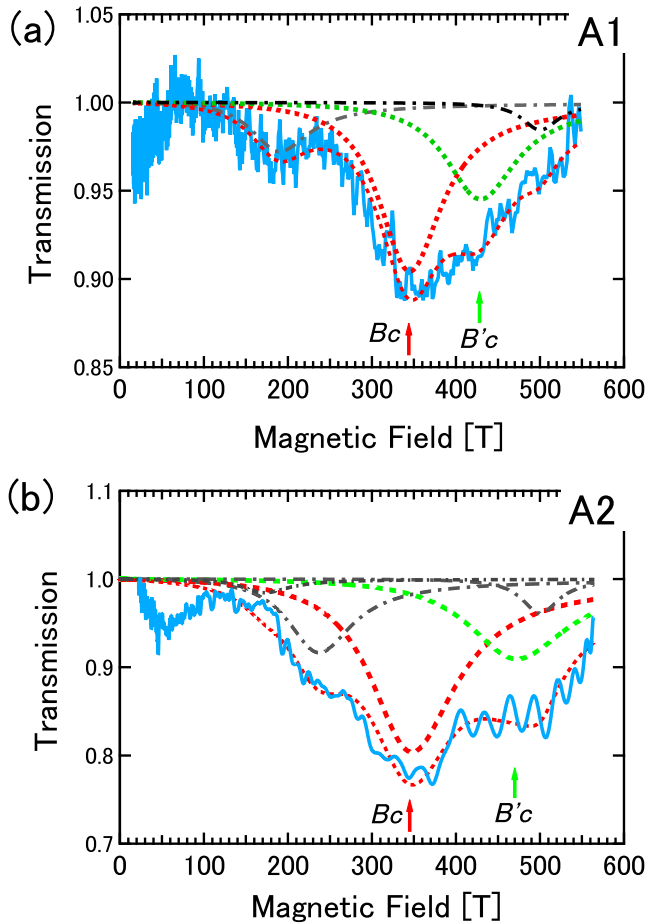


FIG. 3. CR transmission spectra of samples (a) A1 and (b) A2 measured at room temperature in the EMFC magagauss generator. Dashed-dot lines indicate CR contributions from the bilayer graphene mixture in the sample; red- and green-colored dashed lines are the deconvoluted peaks from two splitting CRs with their peak positions,  $B_c$  and  $B'_c$ , respectively. Red dotted lines indicate the total summation of the deconvoluted spectra.

639.1 meV ( $\lambda = 1940$  nm) for A1 and A2, respectively. Due to the random mixture of bilayer fragments in the sample (see Fig. 2 in the Supplemental Material [23]), samples A1 and A2 can be slightly different in the bilayer content.

The final results of the deconvoluted absorption spectra were shown with various peak components by dashed and dotted lines. Results of the deconvoluted CR peaks having the form of Eq. (1) were as follows: (a) sample A1; in the order of increasing magnetic fields: 188 T ( $\tau = 12$  fs), 344 T ( $\tau = 15$  fs), 428 T ( $\tau = 15$  fs), and 500 T ( $\tau = 30$  fs); (b) sample A2: 171 T ( $\tau = 14$  fs), 235 T ( $\tau = 12$  fs), 345 T ( $\tau = 11$  fs), 470 T ( $\tau = 11$  fs), and 500 T ( $\tau = 31$  fs).

Transitions corresponding to the peaks observed at nearly 200 and 500 T in Figs. 3(a) and 3(b) were difficult to assign to any of the allowed CR transition of the intrinsic monolayer graphene. These were contributions from a fragment of the bilayer graphene included in a sample, which were confirmed from CR experimental data and their analysis conducted on bilayer graphene, as can be found in the Supplemental

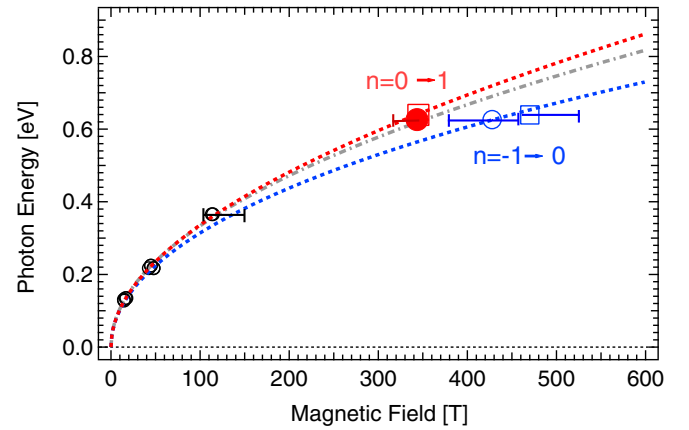


FIG. 4. Landau fan-chart for the CR transitions  $n = -1 \rightarrow 0$  and  $n = 0 \rightarrow 1$ , respectively. The CR peak positions of  $B_c$  and  $B'_c$  in samples A1 and A2 in Fig. 3 are plotted by large-sized symbols. The small-sized symbols under 200 T are the same as those in Fig. 2. The dotted lines are fitted to CR resonance peaks: the red line is for  $n = 0 \rightarrow +1$  and the blue line is for  $n = -1 \rightarrow 0$ . The dashed-dot line represents the extension of the dotted line in Fig. 2 with  $v_F = 0.92 \times 10^6$  m/s.

Material [23]. As several transitions are allowed at around 200 and 500 T in bilayer graphene, and the integrated contributions of those transitions overlap each other, the spectra deconvoluted as bilayer graphene in both figures (depicted by the black dashed-dot lines) were approximated by a Gaussian type function and used for a background of the whole CR spectra. Error estimation and details of the spectral curve fitting carried out in Fig. 3 are presented in the Supplemental Material [23].

Figure 4 displays the CR transition energy vs the magnetic field fan-chart of peak fields  $B_c$  and  $B'_c$  in Figs. 3(a) and 3(b), along with the data in Fig. 1. The main peaks (denoted by  $B_c$ ) at 344 T (sample A1) and 345 T (sample A2) could be regarded as identical transitions within an experimental error and were assigned as arising from  $n = 0 \rightarrow 1$  or  $-1 \rightarrow 0$  CR of a monolayer graphene, judging from the fact that the peaks were roughly positioned on the extended line evolving from a  $\sqrt{B}$  dependence of the low-field  $n = 0 \rightarrow 1$  and  $-1 \rightarrow 0$  CR positions (a dotted line in Fig. 2). Contrastingly, no corresponding CR transition (marked here by  $B'_c$ ) was identified for 428 T (sample A1) and 470 T (sample A2) along the (blue-dashed) line extended simply from the low-field  $\sqrt{B}$  dependence (extended from the dashed line in Fig. 2).

Notably from Fig. 1, the CR absorption spectrum became broader with increasing resonant magnetic fields, mainly caused by the CR peak splitting, which simply appeared as one broad peak smearing out from two broad splitting peaks. Further increase of the magnetic fields until 500 T would result in a visible splitting of the spectra  $B_c$  and  $B'_c$ , as a consequence of the increased peak splitting separation, which attempts to overcome the broadening of each peak (also see Sec. I in Supplemental Material [23]). Therefore, it is a natural consequence to regard  $B'_c$  as a splitting partner of  $B_c$ .

The majority of the previous experimental studies have argued that the observed CR splitting is attributable to the  $e$ - $e$  interaction. They claim that Kohn's theorem should

be inapplicable to the monolayer graphene, which underlies the extreme nonparabolicity of the energy band dispersion. Moreover, they assert that the LL splittings observed in the magnetotransport measurements are induced by the same origin as those observed in the CR spectra [6,8,9,13]. However, these arguments could be reconsidered particularly for the CRs of  $n = 0 \rightarrow +1$  and  $-1 \rightarrow 0$  transitions. It has been revealed that an exact relation holds between the interaction matrix elements (see Eq. (3.10) in Ref. [30]), resulting in the resurgence of Kohn's theorem [30]. Therefore, it should be implausible to conclude that the observed CR splittings are derived simply from the same origin with respect to the  $e$ - $e$  interaction. Thus, in our case, the CR splitting  $B_c$  and  $B'_c$  observed in Fig. 3 cannot be understood as a direct consequence of the LL splittings observed in the magnetotransport measurements [15,16].

We hereby propose the most viable interpretation of the phenomenon. Split peaks  $B_c$  and  $B'_c$  could be regarded as the transitions of  $n = 0 \rightarrow +1$  and  $n = -1 \rightarrow 0$ , respectively, as a result of lifting degeneracy, i.e., breaking of the electron-hole symmetry in the Dirac energy dispersion. The electron-hole asymmetry of the energy band is recognized as quite small and difficult to be observed in monolayer graphene. However, an ultrahigh magnetic field (as high as  $B \sim 400$ – $500$  T) could potentially manifest the CR splitting caused by the electron-hole asymmetry (see Sec. I in the Supplemental Material [23]). To the best of our knowledge, such electron-hole asymmetry observed in CR spectra of a normal monolayer graphene remains unreported except for the case of a strained graphene [31]. As for the bilayer graphene [32,33], the importance of the electron-hole asymmetry of the energy band has already been pointed out theoretically [34].

The CR splitting energy induced by the electron-hole asymmetry mainly stems from the higher-order  $\mathbf{k} \cdot \mathbf{p}$  corrections, namely, the overlapping integral between the nearest-neighbor  $\pi$  orbitals and the hopping integrals between the next-neighbor orbitals. The term is linearly approximated in magnetic field  $B$  [35]. Thus, the CR energies of  $n = 0 \rightarrow +1$  and  $-1 \rightarrow 0$  are modified and given by

$$E_{0 \rightarrow +1} = v_F \sqrt{2e\hbar B} + cB, \quad (2)$$

$$E_{-1 \rightarrow 0} = v_F \sqrt{2e\hbar B} - cB, \quad (3)$$

respectively.

Equations (2) and (3) were fitted to CR peak positions in Fig. 4 with  $v_F = 0.90 \times 10^6$  m/s and  $c = 1.1 \times 10^{-4}$  eV/T, and the results are plotted by dotted lines for the transitions of  $n = 0 \rightarrow +1$  and  $n = -1 \rightarrow 0$ , respectively. Note that simple extrapolation of  $\sqrt{B}$  dependence fitted in magnetic fields lower than 120 T [ $v_F = 0.92 \times 10^6$  m/s] deviates slightly from  $B_c$ , but stays far from  $B'_c$ , which is noticed through the dashed-dotted line in Fig. 4.

As  $n_e = 3 \times 10^{11}$  cm $^{-2}$  and  $B \sim 400$  T yield the low filling factor,  $\nu = 2\pi\hbar n_e/eB \sim 3 \times 10^{-2} \ll 1$ , CR transitions of  $n = 0 \rightarrow 1$  and  $-1 \rightarrow 0$  should have almost the same spectral intensities. Nevertheless, the observed spectra indicate considerably large intensity transfer from the hole CR to the electron CR—the CR intensity of  $n = 0 \rightarrow +1$  is about twice as large as that of  $n = -1 \rightarrow 0$ . This intensity transfer can possibly be induced by mode repulsion between the two CR modes via the  $e$ - $e$  interaction [36], which could have enhanced CR splitting as well.

Finally, we comment briefly on the effect induced by the trigonal warping. In the  $\mathbf{k} \cdot \mathbf{p}$  scheme, the effect of the trigonal warping is proportional to  $(a/\ell)^3$  and could be much smaller than that of the  $B$  linear term proportional to  $(a/\ell)^2$ , where  $a$  is the lattice constant, and  $\ell$  is the magnetic length.

In this study, CR transition peaks of up to approximately 500 T in epitaxial graphene grown on a 4H-SiC(0001) substrate were observed. Ultrahigh resolution was achieved in the CR spectral range of 200–550 T, which led us to observe a CR splitting near 400 T attributed to  $n = 0 \rightarrow +1$  and  $-1 \rightarrow 0$  transitions. The observed CR splitting is interpreted as a consequence of the electron-hole asymmetry of the energy band dispersion caused by the higher-order term in the  $\mathbf{k} \cdot \mathbf{p}$  scheme. An intensity transfer from the electron to the hole CR modes (asymmetry of the CR spectral intensity),  $n = 0 \rightarrow +1$  and  $-1 \rightarrow 0$ , could only be comprehensible via the mode repulsion induced by the  $e$ - $e$  interaction, as has been pointed out in the theory of Asano and Ando [36].

D.N. acknowledges partial financial support from JSPS KAKENHI Grant No. JP26107512. K.A. appreciates the financial support from JSPS KAKENHI Grant No. JP17K05497. S.T. and D.N. are deeply grateful for the useful comments of Prof. Tsuneya Ando.

- 
- [1] K. S. Novoselov, *Rev. Mod. Phys.* **83**, 837 (2011).  
 [2] M. Orlita, C. Faugeras, P. Plochocka, P. Neugebauer, G. Martinez, D. K. Maude, A.-L. Barra, M. Sprinkle, C. Berger, W. A. de Heer, and M. Potemski, *Phys. Rev. Lett.* **101**, 267601 (2008).  
 [3] P. Neugebauer, M. Orlita, C. Faugeras, A.-L. Barra, and M. Potemski, *Phys. Rev. Lett.* **103**, 136403 (2009).  
 [4] M. Orlita, C. Faugeras, R. Grill, A. Wyszomolek, W. Strupinski, C. Berger, W. A. de Heer, G. Martinez, and M. Potemski, *Phys. Rev. Lett.* **107**, 216603 (2011).  
 [5] M. L. Sadowski, G. Martinez, M. Potemski, C. Berger, and W. A. de Heer, *Phys. Rev. Lett.* **97**, 266405 (2006).  
 [6] Z. Jiang, E. A. Henriksen, L. C. Tung, Y.-J. Wang, M. E. Schwartz, M. Y. Han, P. Kim, and H. L. Stormer, *Phys. Rev. Lett.* **98**, 197403 (2007).  
 [7] R. S. Deacon, K.-C. Chuang, R. J. Nicholas, K. S. Novoselov, and A. K. Geim, *Phys. Rev. B* **76**, 081406 (2007).  
 [8] M. Orlita and M. Potemski, *Semicond. Sci. Technol.* **25**, 063001 (2010).  
 [9] E. A. Henriksen, P. Cadden-Zimansky, Z. Jiang, Z. Q. Li, L.-C. Tung, M. E. Schwartz, M. Takita, Y.-J. Wang, P. Kim, and H. L. Stormer, *Phys. Rev. Lett.* **104**, 067404 (2010).  
 [10] A. M. Witowski, M. Orlita, R. Stępniewski, A. Wyszomolek, J. M. Baranowski, W. Strupinski, C. Faugeras, G. Martinez, and M. Potemski, *Phys. Rev. B* **82**, 165305 (2010).

- [11] I. Crassee, J. Levallois, A. L. Walter, M. Ostler, A. Bostwick, E. Rotenberg, T. Seyller, D. van der Marel, and A. B. Kuzmenko, *Nat. Phys.* **7**, 48 (2011).
- [12] L. G. Booshehri *et al.*, *Phys. Rev. B* **85**, 205407 (2012).
- [13] M. Orlita, Liang Z. Tan, M. Potemski, M. Sprinkle, C. Berger, W. A. de Heer, Steven G. Louie, and G. Martinez, *Phys. Rev. Lett.* **108**, 247401 (2012).
- [14] W. Kohn, *Phys. Rev.* **123**, 1242 (1961).
- [15] Y. Zhang, Z. Jiang, J. P. Small, M. S. Purewal, Y.-W. Tan, M. Fazlollahi, J. D. Chudow, J. A. Jaszczak, H. L. Stormer, and P. Kim, *Phys. Rev. Lett.* **96**, 136806 (2006).
- [16] A. F. Young, C. R. Dean, L. Wang, H. Ren, P. Cadden-Zimansky, K. Watanabe, T. Taniguchi, J. Hone, K. L. Shepard, and P. Kim, *Nat. Phys.* **8**, 550 (2012).
- [17] Y. J. Song, A. F. Otte, Y. Kuk, Y. Hu, D. B. Torrance, P. N. First, W. A. de Heer, H. Min, S. Adam, M. D. Stiles, A. H. MacDonald, and J. A. Stroscio, *Nature (London)* **467**, 185 (2010).
- [18] W. A. de Heer, C. Berger, X. Wu, P. N. First, E. H. Conrad, X. Li, T. Li, M. Sprinkle, J. Hass, M. L. Sadowski, M. Potemski, and Gérard Martinez, *Solid State Commun.* **143**, 92 (2007).
- [19] Z. Jin, J. Yao, C. Kittrell, and J. M. Tour, *ACS Nano* **5**, 4112 (2011).
- [20] H. Hibino, S. Tanabe, S. Mizuno, and H. Kageshima, *J. Phys. D: Appl. Phys.* **45**, 154008 (2012).
- [21] H. Hibino, H. Kageshima, F. Maeda, M. Nagase, Y. Kobayashi, and H. Yamaguchi, *Phys. Rev. B* **77**, 075413 (2008).
- [22] S. Tanabe, Y. Sekine, H. Kageshima, M. Nagase, and H. Hibino, *Appl. Phys. Express* **3**, 075102 (2010).
- [23] See Supplemental Material at <http://link.aps.org/supplemental/10.1103/PhysRevB.101.115420> for epitaxial mono-layer graphene sample used for the measurements, the methods for ultra-high magnetic field generation and for cyclotron resonance, and cyclotron resonance peak determination.
- [24] N. Miura, T. Osada, and S. Takeyama, *J. Low Temp. Phys.* **133**, 139 (2003).
- [25] S. Takeyama and E. Kojima, *J. Phys. D: Appl. Phys.* **44**, 425003 (2011).
- [26] D. Nakamura, H. Sawabe, and S. Takeyama, *Rev. Sci. Instrum.* **89**, 016106 (2018).
- [27] D. Nakamura, A. Ikeda, H. Sawabe, Y. H. Matsuda, and S. Takeyama, *Rev. Sci. Instrum.* **89**, 095106 (2018).
- [28] H. Momose, H. Deguchi, H. Okai, N. Mori, and S. Takeyama, *Phys. E (Amsterdam, Neth.)* **29**, 606 (2005).
- [29] D. S. L. Abergel and V. I. Fal'ko, *Phys. Rev. B* **75**, 155430 (2007).
- [30] K. Shizuya, *Phys. Rev. B* **81**, 075407 (2010).
- [31] K.-K. Bai, Y.-C. Wei, J.-B. Qiao, S.-Y. Li, L.-J. Yin, W. Yan, J.-C. Nie, and L. He, *Phys. Rev. B* **92**, 121405 (2015).
- [32] E. A. Henriksen, Z. Jiang, L.-C. Tung, M. E. Schwartz, M. Takita, Y.-J. Wang, P. Kim, and H. L. Stormer, *Phys. Rev. Lett.* **100**, 087403 (2008).
- [33] M. Orlita, C. Faugeras, J. Borysiuk, J. M. Baranowski, W. Strupinski, M. Sprinkle, C. Berger, W. A. de Heer, D. M. Basko, G. Martinez, and M. Potemski, *Phys. Rev. B* **83**, 125302 (2011).
- [34] K. Shizuya, *Phys. Rev. B* **84**, 075409 (2011).
- [35] T. Ando and H. Suzuura, *J. Phys. Soc. Jpn.* **86**, 015001 (2017).
- [36] K. Asano and T. Ando, *Phys. Rev. B* **58**, 1485 (1998).